【論　文】
UDC : 697.11 : 72.011.21 : 551.52 : 628.5
Journal of Architecture, Planning and Environmental Engineering (Transactions of AIJ) No. 372, February, 1987
日本建築学会計画系論文報告集 第 372 号・昭和 62 年 2 月

INVESTIGATION ON THE FORMATION OF THERMAL ENVIRONMENT IN AN URBAN CANYON

——Influence of land covering materials and solar shading by a tree——

by TADAHISA KATAYAMA*, AKIO MORIKAWA**
and SHOICHI MASUDA***, Members of A. I. J.

1. Introduction

Outdoor space of a city is regarded as a succession of urban canyons. Each canyon is characterized by the parameters for urban design; the shape and configuration of buildings, land covering materials. etc[1]. Thermal environment in an urban canyon, which is formed according to these parameters, has a direct influence on the comfort for outdoor activities[2]; from a macroscopic point of view it forms an urban climate[3], and from a microscopic point of view it largely affects the indoor microclimate. However, a few instances of urban design have been interested in the formation of outdoor thermal environment. Fundamental information of the formation of outdoor thermal environment for urban design is much less than that of indoor environment.

As for land covering materials, the surface temperature of materials is supposed to have a considerable influence on thermal environment[4] and several examples of field observation have been reported[5]. The studies of heat balance at the surface are not satisfactory yet though it is decisive of the surface temperature, because some important conditions such as the nature of land covering materials, vegetation and solar shading are not fully considered[6),7]. Several examples of field observation of thermal environment in urban canyons have been reported[8], but no example includes the simultaneous measurement of not only air temperature but also other three thermal factors; namely, globe temperature, humidity and wind speed, and the estimate of a composite thermal index. Effects of vegetation on thermal environment have been variously pointed out. Only a few examples include quantitative measurement of the effects of vegetation; for example, solar shading effects of a single tree[9] or a wisteria trellis[10].

This paper describes the results of field observation about the formation of thermal environment in an urban canyon in the summer with the purpose of acquiring above-mentioned fundamental information for urban design. Influence of land covering materials on the heat balance at the surface is examined on the basis of the field observation. The differences in thermal environment formed above each land covering material and the effects of a shade tree on thermal environment are discussed.

List of symbols

- a : thermal diffusivity, m^2/h
- C_b : emissive constant of a blackbody (=4.88), $kcal/m^2hK^4$
- CO : coefficient of correlation
- G : underground heat flux, $kcal/m^2h$
- H : convective heat flux, $kcal/m^2h$
- L : downward long-wavelength thermal radiation, $kcal/m^2h$
- lE : evaporative latent heat flux, $kcal/m^2h$
- R_{net} : net radiation, $kcal/m^2h$
- r : albedo
- S : global horizontal solar radiation, $kcal/m^2h$

* Dr. Eng., Professor, Kyushu University
** Japan IBM Corp.
*** Graduate Student, Kyushu University
(Manuscript received March 10, 1986)

3247

SET^* : new standard effective temerature of the ASHRAE, °C
T_0 : surface temperature $(=\theta_0+273)$, K
t : air temperature, °C
t_g : globe temperature, °C
t_w : wet-bulb temperature, °C
$\overline{v}$: mean wind speed, m/s
$WBGT$: wet-bulb globe temperature index, °C
X_a : air humidity ratio, kg/kg′
X_0 : saturation humidity ratio at the lawn surface, kg/kg′
Z : depth or height, cm
α : combined heat transfer coefficient $(=\alpha_c+\alpha_r)$, kcal/m²h°C
α_c : convective heat transfer coefficient, kcal/m²h°C
α_r : radiative heat transfer coefficient, kcal/m²h°C
θ_0 : surface temperature, °C
θ_z : temperature of the depth of z cm, °C
ϕ_z : relative humidity, %
ε : emittance
λ : thermal conductivity, kcal/mh°C
ρc : heat capacity, kcal/m³°C

2. Outline of field observation

2.1 The urban canyon

The experimental urban canyon is located in southeast of the city of Fukuoka, about 10 km inland of the bay. Intensive observations have been undertaken during the period 19～22 August 1985 inclusive. The weather has been characterized by continually clear skies with cloudy intervals; that is, typical of the summerly weather.

The experimental work in the field is conducted at three measuring sites as shown in Fig. 1. The canyon is situated between two 5-story buildings and oriented with the along-canyon axis in a north-south direction. The south end opens onto a small street and the north end is enclosed with a 1-story building.

The buildings have some fenestration and the walls are painted with several coats of light-gray paint. The surfaces

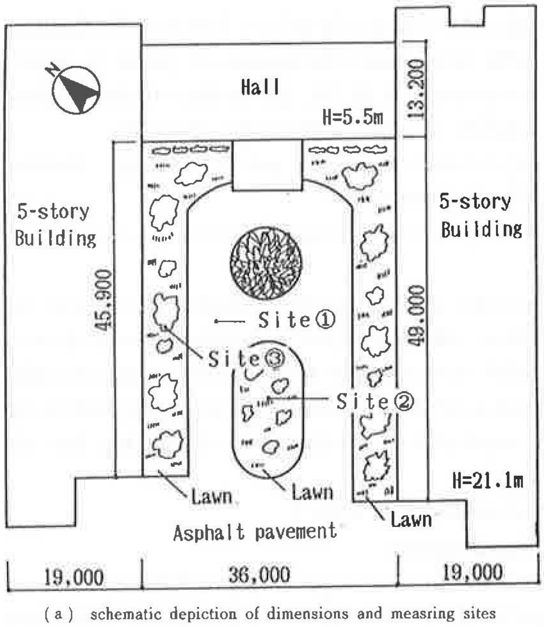

(a) schematic depiction of dimensions and measring sites


(b) actual condition

Fig. 1 The experimental urban canyon

Fig. 2 Actual condition of the shade tree

Table 1 Location and instrumentation of measurement

Item	Method	Height
Solar radiation	Pyrheliometer	Ground level
Air temperature	C-C Thermo-couple(0.05mmϕ)	5,10,30,50,100,150cm
Globe temperature	C-C Thermo-couple(0.1mmϕ) in black globe with a diameter of 15cm	10,30,100cm
Relative humidity	High-polymer Hygrometer	10*,30*,100cm
Wind speed	Super-sonic Anemometer	120cm
	Transistor-type Anemometer	10,30cm
Soil temperature	C-C Thermo-couple(0.1mmϕ)	Ground surface
	C-C Thermo-couple(0.3mmϕ)	2,5,10*cm under ground
Net radiation (Upward,Downward)	Pyrradiometer	20cm

* at the lawn only

of Site ① and Site ② are covered with asphalt and lawn, respectively. Site ③ is located in the shadow in the vicinity of the foot of a singly grown tree whose height and width are about 5 m. Figure 2 shows the situation.

Each measuring site has different duration of sunshine because of the shade by the buildings. The durations are

840~1620 JST at Site ①

900~1720 JST at Site ②

830~1600 JST at Site ③

In comparison with Site ①, the duration at Site ② is longer by 40 minutes, while the duration at Site ③ is shorter by 10 minutes.

2.2 Measurement methods

Two net pyrradiometers are fitted with adaptors on their upper or lower side to measure downward radiation and upward radiation. Using pyrheliometers, global horizontal solar radiation is measured. Above each measuring site air temperatures are measured at six different heights ; 5, 10, 30, 50, 100 and 150 cm above the ground. To reduce the influence of solar radiation and its reflection on air temperature measurement the lengths of the C-C thermo-couples with a diameter of 0.05 mm ϕ are not less than 5 cm[11]. 0.1 mm ϕ C-C thermo-couples are employed to measure globe temperature and surface temperature. Underground temperatures at depths of 2 and 5 cm are measured by 0.3 mm ϕ thermo-couples.

Electric resistance type high-polymer hygrometers are employed to measure the relative humidity. To eliminate the influence of direct solar radiation and others on humidity measurement the sensors are put in Assmann's aspiratory psychrometers and well-ventilated. The humidity is measured at 10, 30, 100 cm above the lawn surface and at 100 cm above the pavement. Vertically uniform humidity is supposed above the pavement.

Data of the above-mentioned items are recorded automatically by a data acquisition system once every 5 minutes. In the figures these data are subsequently reduced to half-hour averages.

A non-contact infrared thermometer is employed to measure the surface temperatures of the buildings and the lawn at recording intervals of 15 minutes during the day.

As for wind direction and wind speed, two-dimentional supersonic anemometers are arranged at 100 cm above the pavement and the lawn surfaces. Their response time is 0.05 second. Wind speed at heights of 10 and 30 cm is measured by transistor-type anemometers. The signals of wind observation are recorded once every 5 seconds.

Due to the number of measuring instruments, the measurement is carried out simultaneously at Site ① and Site ② in the early two days, then the instruments at Site ② are transferred to Site ③. So, in the late two days the simultaneous measurement is carried out at Site ① and Site ③.

The location and instrumentation of the field observation are listed in Table 1.

3. Land covering materials and heat balance at the ground surface

3.1 Radiation, surface temperature, underground temperature, air temperature and humidity ratio.

Solar radiation, net radiation, vertical profiles of air temperature, surface temperature, underground temperature and humidity ratio are taken up as matters of close concernment of the heat balance at the ground surface.

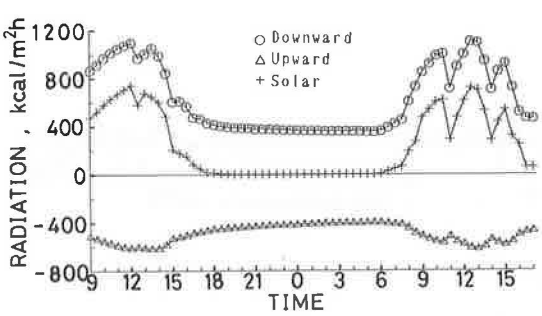

Fig. 3 Downward, upward and solar radition measured at the pavement (Site ①) in the sunshine (19.20 August 1985)

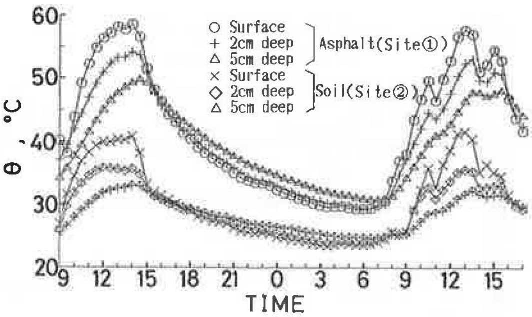

Fig. 4 Surface temperatures and underground temperatures

Figure 3 shows the data of solar radiation, downward and upward radiation at the pavement(Site ①). Atmospheric radiation, solar reflection from the wall surfaces and long-wave radiation are approximately 400 kcal/m²h in total. These values are added to the global horizontal solar radiation in order to obtain the downward radiation. At night, long-wave radiation is constant at 400 kcal/m²h or so. The maximum of upward radiation is approximately 650 kcal/m²h during the day due to the rise in temperature of the asphalt pavement and the solar reflection. At night upward radiation decreases to approximately 400 kcal/m²h according to the drop of the surface temperature.

Figure 4 shows the surface temperatures of the pavement and the lawn, as well as the asphalt and the soil temperatures at depths of 2 cm and 5 cm beneath the surface measuring points. The surface temperature of the pavement is higher than the air temperature by approximately 25°C and the highest value is 60°C. At the depth of 5 cm the asphalt temperature is accompanied with lag time and rises to 50 °C or so. Concerning the lawn, the surface temperature does not often exceed 40°C and the soil temperature at the depth of 5 cm does not exceed 33°C.

Figure 5 shows examples of the vertical profiles of air temperature above the pavement and the lawn. During the day, the difference between the surface temperature and the air temperature at the height of 10 cm is large above the pavement, but the difference above the lawn is very small.

Above the height of 30 cm, the air temperature is almost uniform and no difference is found between the temperatures above the pavement and the lawn. The figure includes the surface temperature of the lawn. It is higher than that of the soil by 5 or 6°C due to the influence of solar radiation but does not exceed 43°C.

The profiles of humidity ratio above the lawn are also shown in Fig. 5. The vertical difference in the humidity ratio near the surface has a peak at midday.

3.2 Net radiation

The net radiation of the ground surface is given by[12)]

$$R_{net}=(1-r)S+\varepsilon L-\varepsilon C_b(T_0/100)^4 \quad (1)$$

Figures 6(a) and 6(b) show the component solar absorption given by each term in Eq. (1) at the pavement and the lawn. To calculate these terms the data of upward radiation and downward radiation, global horizontal solar

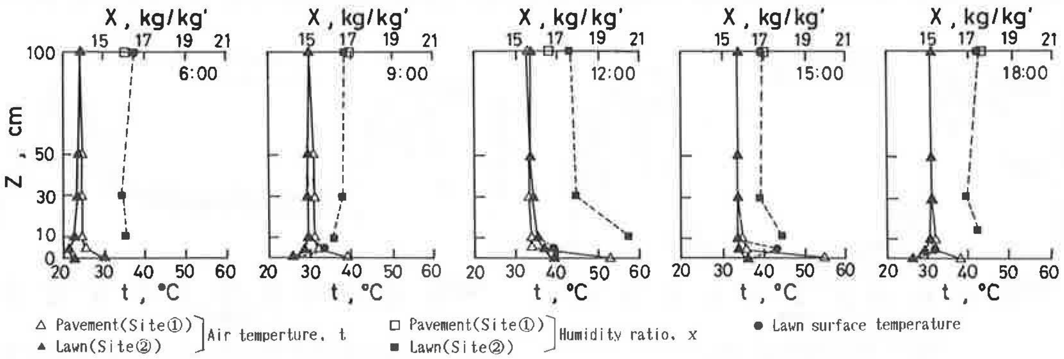

Fig. 5 Profiles of air temperatures and humidity ratios

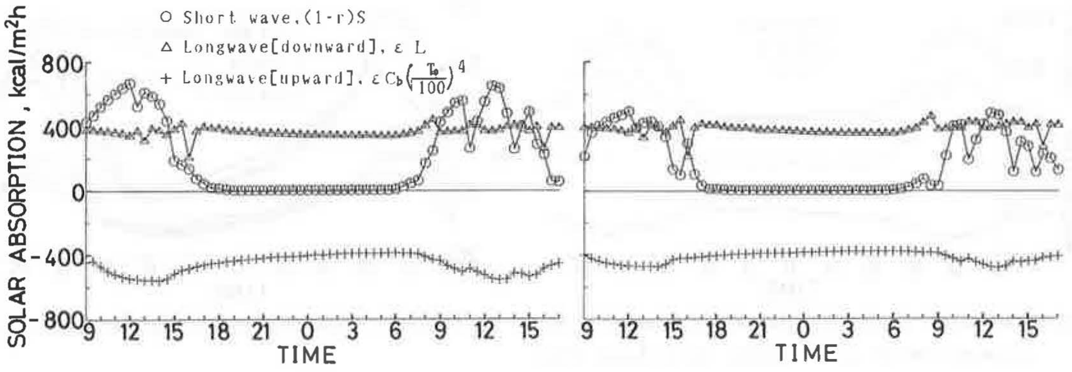

(a) at the pavement (Site ①)　　　(b) at the lawn (Site ②)

Fig. 6 Component solar absorption

radiation and surface temperatures at each measuring site are used, with assumed values of the albedo r and the emittance ε. For the asphalt pavement[13], $r=0.1$ and $\varepsilon=0.95$ are assumed. The sum of the downward radiation and the upward radiation obtained by the measurement as shown in Fig. 3 is similar to the calculated value (shown in Fig. 7). For the lawn, $r=0.3$ and $\varepsilon=1.0$ are assumed.

During the day, the solar absorption of the pavement is greater than that of the lawn by 200 kcal/m²h and below. The upward long-wave radiation of the pavement is also greater than that of the lawn by 100 kcal/m²h and below. The difference becomes smaller at night. Both surfaces have almost identical solar absorption.

Figure 7 shows the net radiation R_{net} obtained by Eq. (1) and Fig. 6 for both surfaces. Due to the differences in the solar absorption and the long-wave radiation, during the day the R_{net} of the pavement is greater than that of the lawn by 100 kcal/m²h or so, but at night it is smaller by 50 kcal/m²h and below.

3. 3 Underground heat flux

In estimating the underground heat flux of the asphalt or the soil, thermal properties of the land covering materials are necessary. Several values based on experiments are available. There are a wide variety of soils, however, and the thermal properties of the soil are largely dependent on the moisture content[15]. The authors of this paper assume the maximum and the minimum values of thermal properties of the asphalt and the soil, based on the conventional data with the elimination of conspicuous exceptions. The generally accepted ones are taken as the representative values. The values are as follows : for the asphalt[13], $a=0.0012$ ($\lambda=0.6$ and $\rho C=500$)~0.0035 ($\lambda=0.7$ and $\rho C=200$) and the representative[14] $a=0.0032$ ($\lambda=0.68$ and $\rho C=211$) ; for the soil, $a=0.0006$ ($\lambda=0.3$ and $\rho C=500$)~0.0030 ($\lambda=1.0$ and $\rho C=300$) and the representative $a=0.0014$ ($\lambda=0.53$ and $\rho C=379$).

With the above-mentioned values, the underground heat flux is calculated by

$$G \fallingdotseq \left(-\lambda\frac{\partial\theta}{\partial z}\right)_z+\rho C\frac{\Delta\bar{\theta}}{\Delta t}z \quad \cdots\cdots (2)$$

where $\Delta\bar{\theta}$ is the mean difference between the surface temperature and the temperature at the depth of z cm. Here the

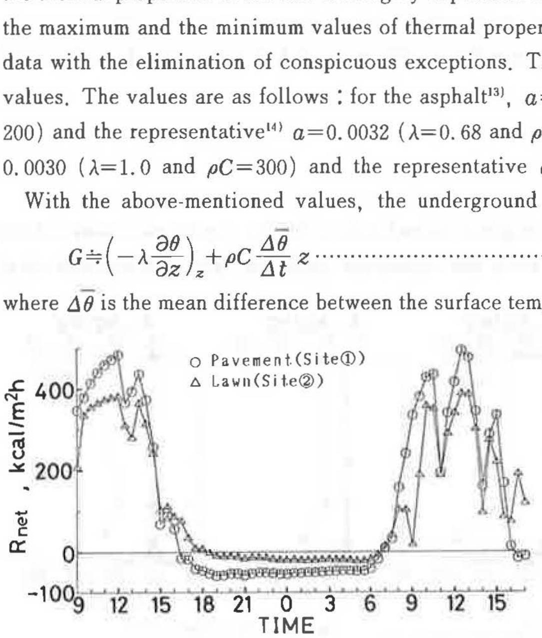

Fig. 7 Net radiations (R_{net})

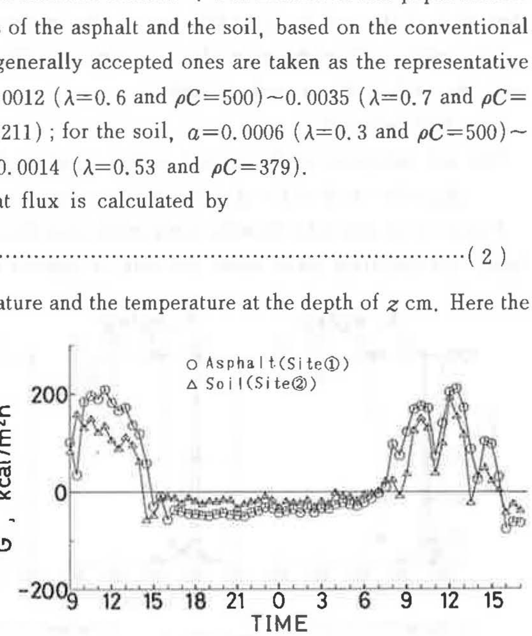

Fig. 8 Underground heat flux (G) in the asphalt (Site ①), and in the soil (Site ②)

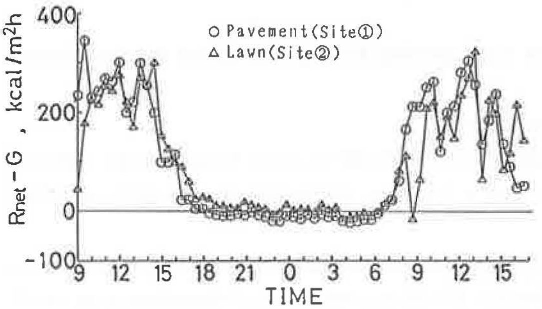

Fig. 9 ($R_{net}-G$) values at the pavement (Site①), and the lawn (Site②)

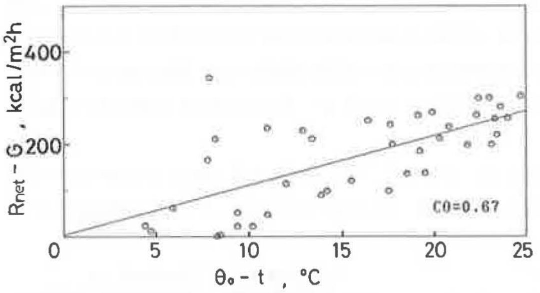

Fig. 10 Relation between (θ_0-t) and ($R_{net}-G$) values at the pavement (Site①)

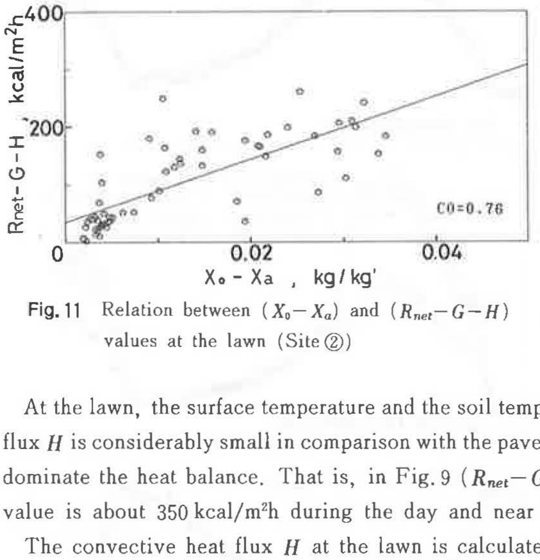

Fig. 11 Relation between (X_0-X_a) and ($R_{net}-G-H$) values at the lawn (Site②)

temperature at the depth of 5 cm is used. By Eq. (2) and Fig. 4, the heat flux in the asphalt is calculated and compared.

As for the asphalt, the value of G varies between 70 and 250 kcal/m^{2}h during the day and between -20 and -70 kcal/m^{2}h at night. For the soil, G varies between 50 and 200 kcal/m^{2}h during the day and between -10 and -30 kcal/m^{2}h at night. The heat flux G based on the representative values of the materials is calculated and shown in Fig. 8. During the day the downward heat flux in the asphalt is about 200 kcal/m^{2}h, on the other hand the downward heat flux in the soil is about 120 kcal/m^{2}h and equivalent to 60 % of the asphalt. At night the upward heat flux in the asphalt is about 40 kcal/m^{2}h, and the upward heat flux in the soil is about 20 kcal/m^{2}h.

3. 4 Convective heat flux and evaporative latent heat flux

With the values in Figs. 7 and 8 the ($R_{net}-G$) values are calculated for the pavement and the lawn. Figure 9 shows the ($R_{net}-G$) values. When it is assumed that the asphalt pavement is dry during the field observation and evaporation from the pavement is negligible[16], the ($R_{net}-G$) value is equivalent to the convective heat flux H. The value of H varies between 200 and 300 kcal/m^{2}h (200 kcal/m^{2}h on the average) during the day according to the rise of the surface temperature. At night H is near to zero. Figure 10 shows the relation between the temperature difference (θ_0-t) and H ($=R_{net}-G$). As for the value of t, the air temperature at the height of 100 cm is representatively used. These two values bear a certain correlation. The coefficient of correlation CO is 0. 67 and the gradient $H/(\theta_0-t)$ is nearly 11.

At the lawn, the surface temperature and the soil temperature do not rise to a high degree, so the convective heat flux H is considerably small in comparison with the pavement, and the evaporative latent heat flux lE is supposed to dominate the heat balance. That is, in Fig. 9 ($R_{net}-G$)=($H+lE$) can be assumed at the lawn. The ($R_{net}-G$) value is about 350 kcal/m^{2}h during the day and near to zero at night as well as at the pavement.

The convective heat flux H at the lawn is calculated by applying the Jürges Equation to the estimate of the convective heat transfer coefficient, by use of the soil surface temperature θ_0 and the air temperature t at 100 cm above it. The value of H is about 60 kcal/m^{2}h during the day. As the soil is covered with the lawn, the convective heat transfer coefficient α_c obtained by using the Jürges Equation is supposed to be overestimated.

Figure 11 shows the relation between the difference in humidity ratio (X_0-X_a) and $lE(=R_{net}-G-H)$ at the lawn, where X_0 is the saturation humidity ratio at the lawn surface temperature and X_a is the humidity ratio of air at the height of 100 cm. These two values bear a certain correlation. The coefficient of correlation CO is 0. 76 and it can be said that lE is relatively proportional to the (X_0-X_a) value[17].

Wind speed varies between 0. 5~3. 0 m/s. Considering that various environmental factors affect heat and mass transfer during the measurement, these coefficients CO will be acceptable. This analysis is expected to develop into practical use.

4. Influence of land covering materials and effects of solar shading by a singly grown tree on thermal environment

4.1 Air temperature, globe temperature and relative humidity

The air temperature, globe temperature and relative humidity at 30 cm and 100 cm above the ground are compared in Fig. 12(a) for the pavement and the lawn both in sunshine, and in Fig. 12(b) for the pavement in sunshine and the lawn with solar shading by a singly grown tree.

Though the air temperature at $Z=30$ cm is sometimes partly higher than the temperature at $Z=100$ cm by 1 or 2°C, the difference is generally small as shown in Fig. 5. The difference in local air temperature at three measuring sites is also small.

The highest globe temperature at the pavement and the lawn in sunshine are almost 45 or 50°C. As for the globe temperatures at $Z=30$ cm during the day, they are higher than those at $Z=100$ cm by 2°C or so at the pavement and by between 2 and 4°C at the lawn. The rise in surface temperature at the pavement and the solar reflection at the lawn can be considered to cause the differences. As for the globe temperatures under the shade tree, they are lower than those in sunshine during the day and do not exceed 40°C. The difference between $Z=30$ cm and $Z \doteq 100$ cm is small. At night they are similar to those at the pavement.

Relative humidity at $Z=30$ cm is not measured at the pavement. The influence of the difference in land covering materials and the height above the ground on relative humidity is small. Diurnal variation of relative humidity is

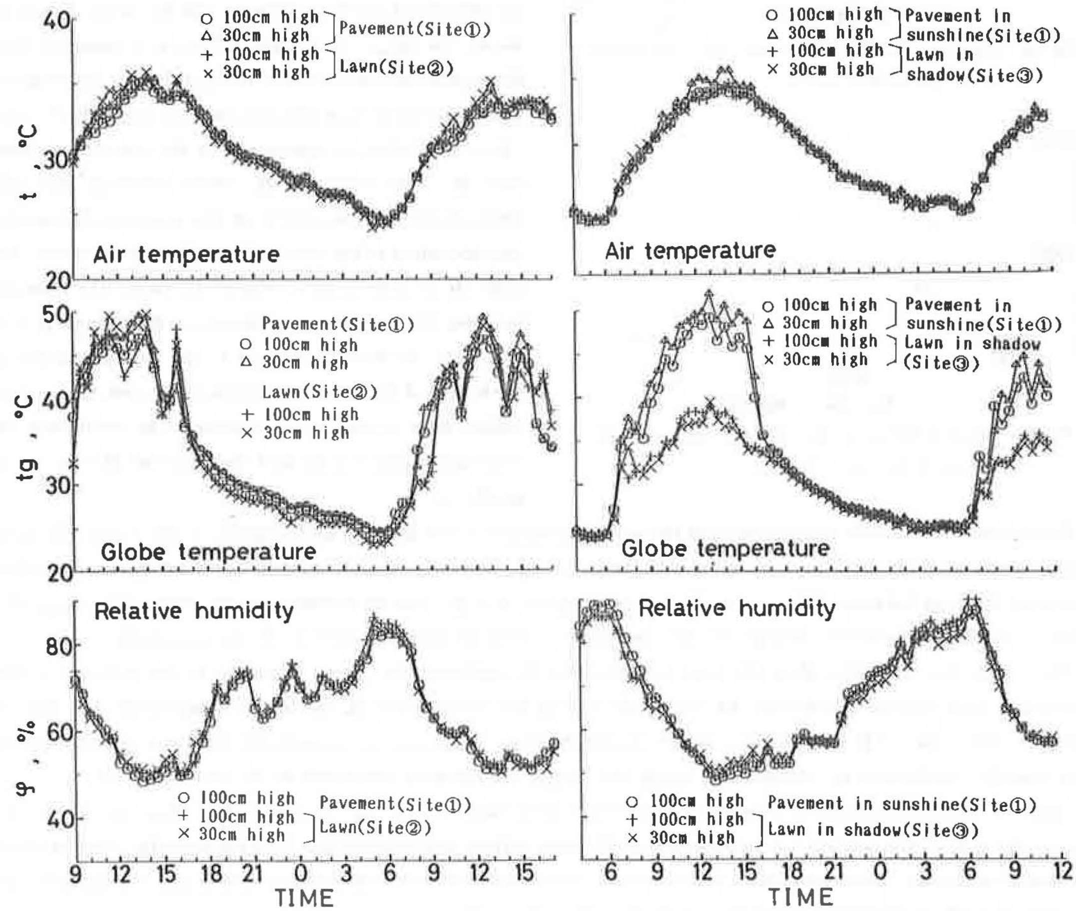

(a) at the pavement (Site③) and the lawn (Site②) both in sunshine (19.20 Aug. 1985)

(b) at the pavement (Site①) in sunshine and the lawn (Site③) in shadow (21.22 Aug. 1985)

Fig. 12 Comparisons of air temperature, globe temperature and relative humidity approximately opposite to that of air temperature. It is low during the day and high at night. It has a minimum value of about 50 % during the day.

4.2 Calculation of globe temperature

For a practical calculation of globe temperature by using the data of temperature, radiation and wind speed, the following equation[18] is available :

$$t_g - t_a = \varepsilon J / (\alpha_c + \alpha_r) \qquad (3)$$

where J is the incoming radiation, $\varepsilon=1$ and $\alpha_r=4.4$ are assumed. Figure 13 shows the difference measured and calculated between globe temperature and air temperature at the pavement and the lawn in sunshine and under the shade tree. As a whole the calculations are close to the measured values. Especially for the globe exposed to direct solar radiation the globe temperatature can be predicted within an error of 0.5°C. The difference between the measured and the calculated values under the tree is about 1.5°C and it may be attributed to sunbeam through the leaves and the location of the pyrheliometer and the globe.

4.3 Overall thermal index

(1) Wet-bulb globe temperature index based on the data

People usually realize that solar radiation has considerable effects on thermal sensation in outdoor space. Information on overall thermal indexes at a location exposed to direct solar radiation is little, while there are several indexes for an air-conditioned room. The authors take up the wet-bulb globe temperature index (*WBGT*) which aims at the protection of sunstroke during army training and has appreciable use as a thermal index under hot conditions[19]. The *WBGT* is decided mainly by the wet-bulb temperature t_w and the globe temperature t_g as follows :

$$\left.\begin{array}{ll} WBGT = 0.7\,t_w + 0.2\,t_g + 0.1\,t & \text{(for the location exposed to direct solar radiation)} \\ WBGT = 0.7\,t_w + 0.3\,t_g & \text{(for the location without direct solar radiation).} \end{array}\right\} \qquad (4)$$

The data of t_w, t_g and t at the height of 100 cm shown in Fig. 12 are substituted into each term of Eq. (4) to calculate the *WBGT*. The *WBGT*'s at the pavement and the lawn in sunshine are shown in Fig. 14(a), and the *WBGT*'s at the pavement in sunshine and at the lawn in shadow are shown in Fig. 14(b).

During the day the *WBGT* at the lawn in sunshine is sometimes higher than that at the pavement by 1°C or so. It is

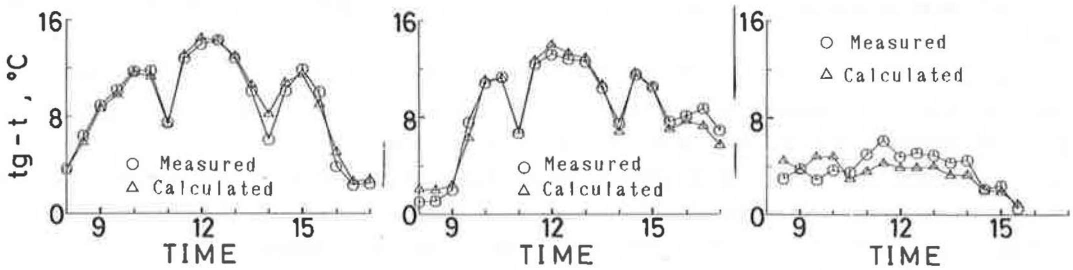

(a) at the pavement (Site①) in sunshine (b) at the lawn (Site②) in sunshine (c) at the lawn (Site③) in shadow

Fig. 13 Difference measured and calculated between globe temperature and air temperature

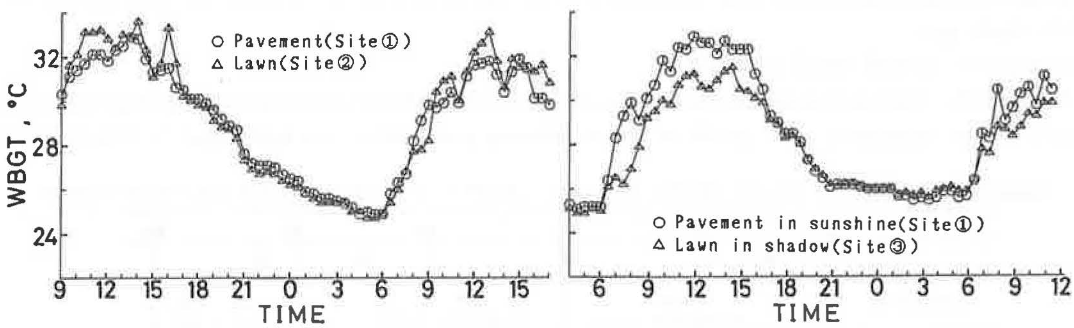

(a) at the pavement (Site①) and the lawn (Site②) both in sunshine (b) at the pavement (Site①) in sunshine and the lawn (Site③) in shadow

Fig. 14 Comparison of wet-bulb globe temperture (*WBGT*) attributed to the difference in solar reflection and the slight difference in humidity. At night the *WBGT* at the pavement is slightly higher than that at the lawn. The *WBGT* at the lawn in shadow is lower than that at the pavement in sunshine by 2°C or so during the day. That implies an appreciable effect of solar shading. After sunset and at night the *WBGT*'s at both measuring sites are similar.

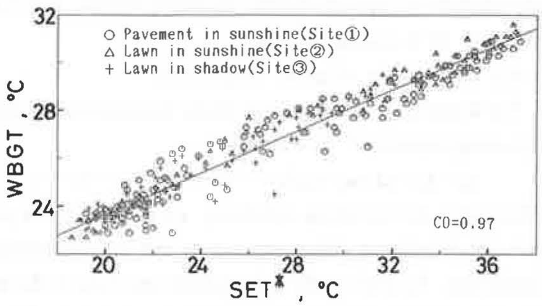

Fig. 15 Relation between new standard effective temperature of the ASHRAE (*SET**) and wet-bulb globe temperature index (*WBGT*)

The new effective temperature[20] takes account of physiological reactions of a human body such as mean skin temperature, skin wettedness and heat dispersion toward the surroundings, and has wide use as a new criterion of themal environment in an air-conditioned room in America. The authors bring in an imaginary standard conditon where $\phi=50$ %, $\bar{v}=0.1\sim0.15$ m/s, the intrinsic clo level=0.6 and the level of activity=1.1 met are assumed[20]. The new standard effective temperature of the ASHRAE, *SET**, is calculated under the condition described above and compared with the *WBGT*. The data obtained by the experimental work are used to calculate the *SET**. In the calculations the intrinsic clo level=0.3 and the level of activity=1.2 met are assumed for the actual situation. Figure 15 shows the relation between the *SET** and the *WBGT* obtained by using the data at 100 cm above the ground.

The *WBGT* and the *SET**, obtained by using the data of thermal factors at the pavement, at the lawn in sunshine and under the shade tree, bear a fairly close correlation. The coefficient of correlation *CO*=0.97. The *SET** varies between 18 and 38°C, while the *WBGT* varies between 22 and 32°C. These two values are adequately expressed by a linear equation.

Table 2 shows reference of the *SET** to temperature sensation and comfort sensation[21]. According to the investigation on outdoor thermal environment and people's activity in several apartment and others, the situation of *SET**=35°C seems to be a criterion of outdoor activity[22]. Here the value of *WBGT* for *SET**=35°C is equivalent to 30°C.

It seems indeliberate to relate the *SET** with the *WBGT*, since they are based on different design and calculations. The close correlation between the two are interesting, however. The relations between these two indexes and outdoor thermal sensation should be clarified in the future.

On the assumption that the effect of the shade by the buildngs is small between 900 and 1600 JST, data from another period are omitted from analysis in order to examine the frequency of each level of the *WBGT* at the three measuring sites. Figures 16(a) and 16(b) present the results in the form of histogram.

The mean *WBGT* at the lawn in sunshine is higher than that at the pavement by 0.5°C or so. At the rate between 40 and 50 % the *WBGT* at the both sites exceeds 30°C. On the other hand the mean *WBGT* under the shade tree is lower than that at the pavement by 1.5°C or so, and exceeds 30°C at the rate of 5 % or so. It implies the solar shading effect of the shade tree.

(2) Influence of wind speed on *WBGT*

Wind speed is dependent on the location. Especially in an urban canyon situated between buildings such as the canyon of this experiment, wind speeds at two neighboring points differ to a high degree[23]. Simultaneously

Table 2 Reference of new standard effective temperature (*SET**) to temperature sensation and comfort sensation

SET*(°C)	15	20	25	30	35	40
temperature sensation	cool	slightly cool	neutral	slightly warm	warm	hot / very hot
comfortable sensation	slightly uncomfortable		comfort		uncomfortable	very uncomfortable

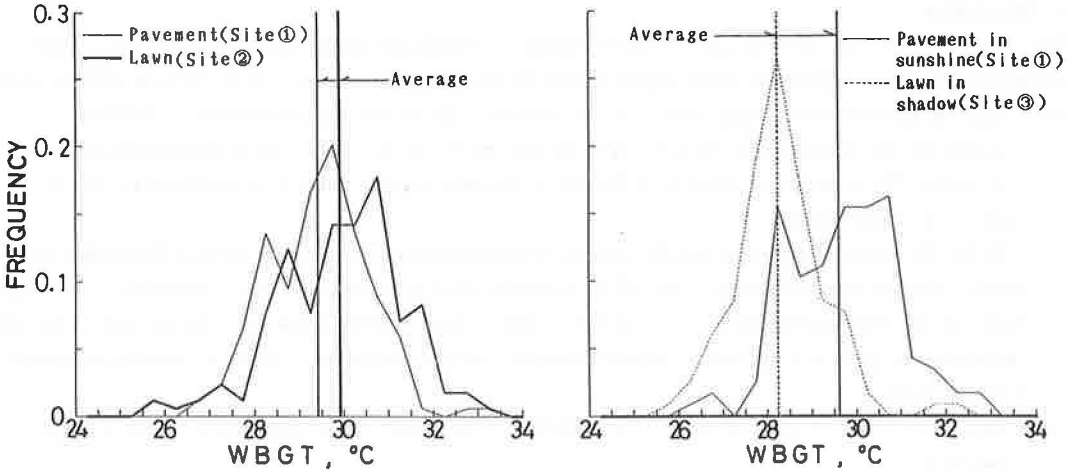

(a) at the pavement (Site①) and the lawn (Site②) both in sunshine

(b) at the pavement (Site①) in sunshine and the lawn (Site③) in shadow

Fig. 16 Histogram of wet-bulb globe temperature index (*WBGT*)

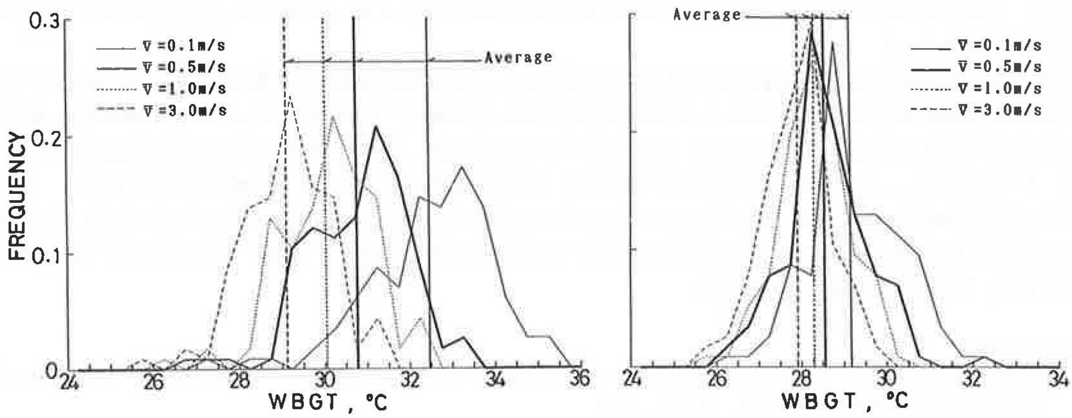

(a) at the pavement (Site①) in sunshine

(b) at the lawn (Site③) in shadow

Fig. 17 Histogram of wet-bulb globe temperature index (*WBGT*) for various wind speeds

measured wind speeds at Site ① and Site ②, or at Site ① and Site ③ differ to a considerable degree. The difference in wind speed has influence on the globe temperature and the thermal sensation.

To estimate the influence of the wind speed on the *WBGT*, four different wind speeds are assumed ; 0. 1, 0. 5, 1. 0, and 3. 0 m/s. Then the convective heat transfer coefficient for each wind speed is obtained as 2. 8, 6. 3, 9. 0 and 15. 6 kcal/m²h°C, respectively, according to Ref. (24). The globe temperatures are calculated by using the data of the measurement and substituting the newly obtained convective heat transfer coefficients into Eq. (3) in stead of the convective heat transfer coefficient for the actual wind speed. The *WBGT* is subsequently calculated by substituting the newly obtained globe temperatures into Eq. (4). The period for the calculations is between 900 and 1600 JST. Figures 17(a) and 17(b) are the histograms of the *WBGT* for various wind speeds. In Fig. 17(a) the histogram of the *WBGT* at the pavement in sunshine is drawn. For $\overline{v}$=0. 1 m/s ; i. e. under windless conditions, the mean *WBGT* is 32. 5°C. For $\overline{v}$=0. 5 m/s the mean *WBGT* drops by 1. 7°C or so. As the wind speed becomes higher, the mean *WBGT* becomes lower, but the change is decelerated.

In Fig. 17(b) the histogram of the *WBGT* under the shade tree is drawn. The mean *WBGT* is 29. 2°C for $\overline{v}$= 0. 1 m/s and 27. 9°C for $\overline{v}$=3. 0 m/s. The influence of the wind speed on the *WBGT* is little in shadow as compared with sunshine. The *WBGT* exceeds 30°C at the rate of 30 % or so for $\overline{v}$=0. 1 m/s and 10 % and less for $\overline{v}$=0. 5 m/s. Effects of slight wind are appreciable.

5. Conclusions

The surfaces of the experimental urban canyon consist of asphalt pavement, lawn and vegetation. Intensive observations have been undertaken under typical summerly weather conditions to clarify the heat balance at the surfaces and the thermal environment formed in the canyon. The results are summarized as follows :

(1) During the day the convective heat flux H at the pavement is great and it is relatively proportional to the ($\theta_0 - t$) value. The evaporative latent heat flux lE at the lawn is great and it is proportional to the ($X_0 - X_a$) value to a certain degree.

(2) As for the daytime heat balance at the surface, at the pavement approximately 60 % of the midday radiant surplus is lost as sensible heat to the air and the remaining 40 % is stored in the canyon materials. On the other hand, at the lawn approximately 15 % of the midday radiant surplus is lost as sensible heat to the air, approximately 35 % is stored in the canyon materials, and the remaining 50 % is consumed by evaporation from the lawn.

(3) Regardless of direct solar radiation, the *WBGT* and the *SET** in the urban canyon bear a fairly close correlation.

(4) Influence of land covering materials on the overall thermal indexes is little ; the difference in the *WBGT* is 0.5°C or so. Effect of solar shading by a tree is great ; the *WBGT* under the shade is lower than that in sunshine by 1.5°C or so and exceeds 30°C at a low rate.

(5) Effect of wind speed on the sensation of a human body is great in sunshine as compared with shadow.

Acknowledgement

The experimental work was supported by Mr. M. Hashida, a graduate student of Kyushu University, and Mr. M. Morodomi and Miss S. Kido, students of Kyushu Institute of Design. The use of several instruments was realized by the help of Dr. A. Ishii. Their support is gratefully acknowledged. The authors wish to record appreciation to Mr. T. Nakashima, a student of Fukuoka University, for his valuable help in completing this paper.

This study participates in the special project research on natural energy (complex use of natural energy, the head researcher is Professor K. Kimura, Waseda University) under the grant in aid of scientific research of the Ministry of Education, Science and Culture, Japan.

References

1) Ojima, T. and Miura, M. : Classification of Exterior Space Composition and Pilot Measurement of Their Thermal Environment, Transactions of AIJ, No. 335, 1984

2) Yamaguchi, K. and Kobayashi, Y. : Heat Exchange by Radiation Including Insolation between Human Body and Overall Outdoor Environment Including Buildings, Ground and Sky, Japanese Journal of Biometeorology, Vol. 17, No. 1, 1980

3) Naito, K., Mizuno, M. and Urushizaki, N. : Urban Canyons as a Factor for Formation of Urban Climate, Transactions of the Society of Heating, Air-Conditioning and Sanitary Engineers of Japan, No. 22, 1983

4) Enman, R. : Distribution of Incident Solar Radiation and Temperature of Ground Surface Surrounded by Buildings, Transactions of the Society of Heating, Air-Conditioning and Sanitary Engineers of Japan, No. 24, 1984

5) Naito, K., Mizuno, M. and Yamawaki, H. : Effects of Surrounding Land Covers on Local Thermal Environment—Survey in Japan Expo. Park—, Transactions of the Society of Heating, Air-Conditioning and Sanitary Engineers of Japan, No. 25, 1984

6) Nunez, M. and Oke, T.R. : The Energy Balance of an Urban Canyon, Journal of Applied Meteorology, Vol. 16, 1977

7) Ojima, T. and Moriyama, M. : Applied Study of Earth Surface Heat Budget's Theory for Regional Environmental Assessment, Transactions of AIJ, No. 265, 1978

8) Nakamura, Y., Hiraoka, H., Nishimura, K. and Yoshida, A : Experiment on Control of Thermal Environment in a Two-Dimensional Rectangular Cavity Space, Summaries of Technical Papers of Annual Meeting, Kinki Chapter of AIJ, 1984

9) Hoyano, A. and Hamaguchi, N. : Shading Effects of a Single Canopy and Thermal Environment Under the Tree, Summaries of Technical Papers of Annual Meeting of AIJ, 1984

10) Hoyano, A. and Kusumoto, A. : Effects of Wisteria Trellis on Solar Control, Summaries of Technical Papers of Annual Meeting of AIJ, 1985

11) Nakamura, Y., Hiraoka, H. and Nishimura, K. : Experiment of Air Temperature Distribution in Urban Canyon, Technical Papers of Environmental Engineering of AIJ, No. 1, 1985

12) Kondo, J. : A Guide for the Study on Heat Balance of Complex Terrain with Various Ground Surfaces, Journal of Meteorological Society of Japan, Vol. 31, No. 9, 1984

13) Katto, Y. : An Introduction of Heat Transfer, Yoken-Do, 1981
14) Narita, K., Sekine, T. and Mitsudera, M. : The Observation of Heat Balance at the Surface of Asphalt Pavement (Field Experiment Using Test Block), Transactions on Environmental Engineering in Architecture of AIJ, No. 5, 1983
15) Nakajima, Y., Ohashi, K. and Amano, K. : Study of Thermal Conductance of Earth, Summaries of Technical Papers of Annual Meeting of AIJ, 1980
16) Narita, K. and Mitsudera, M. : Measurement of Evaporation from Earth Surface, Science of Environmental Information, 10-3, 1981
17) Kondo, J. : Science of Atmospheric Boundary Layer, Tokyo-Do Shuppan K. K., 1983
18) Saito, H. : Architectural Climate, Kyoritsu Shuppan K. K., 1974
19) Yaglou, C. P. and Minard, C. D. : Control of Heat Casualties at Military Training Centers, American Medical Association, Archives of Industrial Health, Vol. 16, 1957
20) Gagge, A. P., Nishi, Y. and Nevins, R. G. : The role of Clothing in Meeting Fea Energy Conservation Guidelines, ASHRAE Transactions, 1976 II
21) Gagge, A. P. and Nishi, Y. : Heat Exchange between Human Skin Surface and Thermal Environment, Handbook of Physiology, Reactions to Environmental Agents, American Physiological Society, 1977
22) Hirokawa, Y. and Horie, G. : Thermal Sensory Environment and Human Behavior in the System of Indoor and Outdoor Living Spaces, International Symposium of the Impact of Climate on Planning and Building, IFHP, 1980
23) Morikawa, A., Katayama, T., Nishida, M., Ishii, A. and Tsutsumi, J. : Study on Formation of Thermal Environment in Urban Canyon, Summaries of Technical Papers of Annual Meeting, Kyushu Chapter of AIJ, 1985
24) Holman, J. P. : Heat Transfer, Fifth edition, McGraw-Hill International Book Co. 1981
[already published papers relating to this article]
25) Masuda, S., Nakashima, T., Morikawa, A., Katayama, T. and Ishii, A. : Investigation on Thermal Environment in an Urban Canyon, No. 1-3, Summaries of Technical Papers of Annual Meeting, Kyushu Chapter of AIJ, 1986

【論　文】
UDC : 697.11 : 72.011.21 : 551.52 : 628.5

日本建築学会計画系論文報告集
第 372 号・昭和 62 年 2 月

建築外部空間の熱環境形成に関する調査研究（梗概）

——地表面被覆材料および樹木による日射遮蔽の影響——

正会員　片　山　忠　久*
正会員　森　川　明　夫**
正会員　増　田　正　一***

1. 緒　言

建物に挟まれた外部の空間に形成される熱環境は，直接的には屋外活動の快適性を左右し[2]，マクロには都市気候を形成する単位となり[3]，またミクロにはシェルターを通して室内気候に大きな影響を及ぼす。この建築外部空間の熱環境は，日射，風等の自然エネルギーの作用と建物の形態，配置，方位および地表面被覆材料等の設計計画上のパラメータによって形成される[1]。しかし，このような熱環境の形成を対象とした建築外部空間の設計事例は少なく，またその設計のための基礎資料も，室内環境のそれに比べて非常に乏しいのが現状である。

設計パラメータの１つである地表面の被覆材料に関しては，その表面温度が熱環境に及ぼす影響は非常に大きい[4]と考えられ，いくつかの実測例がすでに報告されている[5]。しかし地表面の熱収支に関する研究は，被覆材料の種類，表面の植栽の状態や日射遮蔽の程度等，多くの条件を考慮すればまだ十分とはいい難い[6),7]。また建築外部の熱環境の実測例もいくつか報告されいるが[8]，気温のみではなくグローブ温度，湿度および風速の温熱四要素を測定し，総合的な温熱指標まで計算した例は無いようである．熱環境に対する植栽の効果については種々指摘されいるけれども，その定量的な測定例は少なく，単木樹[9]や藤棚[10]による日射遮蔽の効果に関する測定例が２，３報告されている程度である。

本稿は，上記のような設計上の基礎資料を得ることを目的として，建築外部空間における夏季の熱環境形成の実態を調査した結果について述べるものである。この調査ではまず，地被材料による表面熱収支の相違を実測結果に基づいて考察する。次に各地被材料の上に形成される熱環境の差および単木樹による日射遮蔽が熱環境に及ぼす効果について検討する。

2. 実測の概要

東西を５階建，北側を１階の建物で囲われた中庭に，Fig. 1 に示す３つの測定点を設け実測を行う。測定点①はアスファルト面，測定点②は芝地面である。Fig. 2 に示す単木樹の陰に測定点③を選ぶ。

気温は日射等の影響を除くため，直径 0.05 mm ϕ，裸線部長さ 5 cm の *C-C* 熱電対により測定する[11]。グローブ温度と地表面温度の測定には 0.1 mm ϕ の、地中温度の測定には 0.3 mm ϕ の *C-C* 熱電対を使用する。建物壁面や芝表面の温度は非接触型放射温度計により測定する。

相対湿度の測定は，高分子素子使用電気抵抗型湿度計をアスマン通風温湿度計の中に設置し通風の状態で行う。

各測定点の地上高さ 100 cm における風向・風速は二次元超音波風速計，地上 10 および 30 cm の風速は無指向性熱式微風速計によって測定する。以上を Table 1 に示す。

3. 地表面被覆材料と表面熱収支

Fig. 3 に測定点①のアスファルト面における放射の実測値を示す。下向きの全放射量は，水平面全天日射量に約 400 kcal/m²h の大気放射，壁面からの反射日射と長波放射が加わったものになっている。上向きの全放射量は，日中の最大値で 650 kcal/m²h になり，夜間は表面温度の下降とともに約 400 kcal/m²h 程度まで減少する。

Fig. 4 にアスファルトと芝地の表面および地中温度を比較して示す。地表面および地中温度ともにアスファルトが芝地に比べ約 20°C 高くなっている。

Fig. 5 はアスファルト面上および芝地面上の気温の垂直分布を比較している。日中表面温度の差は大きいけれども，地上 30 cm 以上の高さの気温はほとんど一定である。

Fig. 6 (a) および (b) はそれぞれアスファルト面と芝地面の，Eq. (1)[12]右辺各項で示される成分別放射吸収熱量を示す。日中アスファルト面の日射吸収量は芝地面に比較して最大約 200 kcal/m²h 大きく，上向き長波長放射量も最大 100 kcal/m²h 程度大きい。長波長放射

* 九州大学　教授・工博
** 日本 IBM 株式会社・工修
*** 九州大学　大学院生
（昭和 61 年 3 月 10 日 原稿受理）

の吸収量は両面においてほとんど等しい。

Fig. 7 に各面の放射収支 R_{net} を比較して示す。日中はアスファルト面の R_{net} が約 100 kcal/m^{2}h 芝地面より大きく，逆に夜間は最大 50 kcal/m^{2}h 程度小さくなる。

Fig. 8 はアスファルト面と芝地面の地中伝熱量を示す。熱物性値，特に土のそれは非常に多種多様である[15]が，ここでは一般に良く使用される代表的な値を採用している[13),14]。日中はアスファルト面で約 200 kcal/m^{2}h の下方への伝熱量があるのに対し，芝地面では 120 kcal/m^{2}h 程度である。夜間は上向きの伝熱量が芝地面で約 20 kcal/m^{2}h に対しアスファルト面で 40 kcal/m^{2}h 程度である。

Fig. 9 はアスファルト面と芝地面の $(R_{net}-G)$ を示す。アスファルト面からの蒸発は無視できるので[16]，$(R_{net}-G)$ は対流熱伝達量 H となる。H と（アスファルト表面温度 θ_0—気温 t）との関係を求めれば Fig. 10 のごとくであり両者の相関は比較的高い。

一方，芝地面において風速の測定値および Jürges の式を使って対流熱伝達量 H を求めれば，日中の最大値 60 kcal/m^{2}h 程度である。蒸発潜熱量 $lE=R_{net}-G-H$ と（芝表面温度の飽和絶対湿度 X_0－地上 1 m の絶対湿度 X_a）の関係を求めれば Fig. 11 ごとくである。

4. 熱環境に及ぼす地被材料の影響と単木樹による日射遮蔽の効果

気温，グローブ温度および相対湿度の実測値を，日向のアスファルト面と芝地面とで比較して Fig. 12(a) に，日向のアスファルト面と単木樹による樹陰とで比較して Fig. 12(b) にそれぞれ示す。気温や相対湿度に比べてグローブ温度の条件による相違が大きい。特に樹陰のグローブ温度は，日中，日向のそれに比べ 10°C 以上低い。

Fig. 13 はグローブ温度と気温の差 (t_g-t) を Eq. (3) および放射量と風速の測定値から計算[18]し，実測値と比較したものである。日向での両者は±0.5°C 以内で一致している。樹陰において両者の差がやや大きいのは，日射計とグローブ温度計に対する木洩日の差と考えられる。

直達日射のある場における総合的な温熱指標として湿球グローブ温度指数 $WBGT$[19]を採り上げ Eq. (4) から求める。

Eq. (4) および Fig. 12 から地上 100 cm の $WBGT$ を計算し，日向のアスファルト面と芝地面を比較して Fig. 14(a) に，日向のアスファルト面と樹陰を比較して Fig. 14(b) に示す。

Fig. 15 は実測値に基づく $WBGT$ と SET^*[20]の相関を示すが両者の相関は非常に高い。

Fig. 16(a) および (b) は，9：00～16：00 における Fig. 14(a)，(b) の $WBGT$ の頻度分布を求めたものである。日向の芝地面における $WBGT$ の平均値はアスファルト面に比べ約 0.5°C 高い。一方，樹陰の $WBGT$ の平均値は日向のアスファルト面に比べ約 1.5°C 低い。

各測定点において同一の一定風速が吹くものとし，これと放射，表面温度の実測値を使用して Eq. (3) からグローブ温度 t_g を計算する。この計算された t_g と湿球温度 t_w，気温 t の実測値を使用し，Eq. (4) から各面の $WBGT$ を計算する。風速のみを 0.1，0.5，1.0 および 3.0 m/s の 4 段階に変化させて，その $WBGT$ への影響を調べる。このようにして計算した 9：00～16：00 における $WBGT$ の頻度分布を各面について比較し Fig. 17(a) および (b) に示す。Fig. 17(a) は日向のアスファルト面における $WBGT$ の頻度分布であり，風速の影響が大きい。一方，Fig. 17(b) は樹陰における $WBGT$ の頻度分布であるが，風速の影響は日向のアスファルト面における程顕著ではない。

5. 結果のまとめ

(1) 日中，アスファルト面の対流熱伝達量は大きく，(表面温度—気温）との相関が比較的高い。芝地面の蒸発潜熱量についても（表面温度の飽和絶対湿度—地上 1 m の絶対湿度）との相関が比較的高い。

(2) 日中の熱収支は，アスファルト面：$G/R_{net}=0.40$，$H/R_{net}=0.60$ である。一方，芝地面：$G/R_{net}=0.35$，$H/R_{net}=0.15$，$lE/R_{net}=0.50$ である。

(3) 屋外における $WBGT$ と SET^* は，直達日射の有無によらず，非常に高い相関関係がある。

(4) 地上 1 m における熱環境指標に及ぼす地被材料の影響は小さく $WBGT$ の差で 0.5°C 程度である。樹木の日射遮蔽効果は大きく，日向に比べ $WBGT$ で 1.5°C 低下し，$WBGT$ が 30°C を超過する割合も小さい。

(5) 風速が体感に及ぼす効果は，樹陰に比べ日向において大きい。